Journal of the European Ceramic Society 17 (1997) 781–787
PII: S0955-2219(96)00138-0

0955-2219/97/$17.00

X-Ray Data for New Y–Si–Al–O–N Glass Ceramics

K. Liddell, H. Mandal & D. P. Thompson

Materials Division, Department of Mechanical, Materials & Manufacturing Engineering, University of Newcastle, Newcastle upon Tyne, UK

(Received 18 April 1996; accepted 23 July 1996)

Abstract

Since the 1970s an increasing number of crystalline oxynitrides have been observed as grain boundary phases in sialon ceramics. In particular, the well-known four- and five-component phases in the Y–Si–Al–O–N system have been accepted as the total picture in this system and the potential for new phases has not been considered. However, with further development of sialon glasses and glass ceramics, post-preparative heat-treatment has revealed a number of previously uncharacterised crystalline phases occurring particularly at temperatures below 1200°C. Three such phases are discussed, I_w, Q and D, all of which have been observed previously by other researchers but without X-ray diffraction data; Q-phase occurs in some rare earth as well as yttrium sialon systems. All these phases can be produced only within a limited temperature range and are critically dependent on starting composition and heat-treatment temperature, so the present data will complement those already existing for devitrified sialon glass products, with potentially more phases yet to be identified.

1 Introduction

Figure 1 shows the well-established crystalline phases in the Y–Si–Al–O–N system. It can be seen that there are no ternary Y_2O_3–Al_2O_3–SiO_2 compounds, nor any quaternary Y–Al–O–N phases. Those that do occur lie either along the Y_2O_3–Al_2O_3 join or are formed in the Y–Si–O–N system, with the associated ranges of solid solution into the five-component system formed by Si,Al and O,N substitution. The only five-component phase hitherto established in the Y–Si–Al–O–N system is Y_2SiAlO_5N, known as B-phase, which lies along the line joining $YSiO_2N$ and $YAlO_3$, and is found at temperatures below 1150°C. It was originally studied by Rae[1] and was thought to be a point composition; later results, however, showed it to be part of a solid solution extending approximately from 40–70 mol% $YAlO_3$.[2] In contrast to $MSiO_2N$-type wollastonites (M=Y,Ln), B-phase exhibits perfect hexagonal symmetry without stacking faults, and unit cell dimensions are plotted in Fig. 2. Crystalline B-phase can be prepared together with some residual glass, from more SiO_2-rich compositions in the glass-forming region. Heat treatment studies have been carried out and are reported elsewhere,[3] but it has been observed that as B-phase decomposes, a second, apparently structurally related, phase occurs alongside it or with accompanying wollastonite. This phase, designated I_w, was first observed using SEM techniques by Leng-Ward & Lewis[4,5] as a result of heat treating Y–Si–Al–O–N glasses, particularly those with composition $Y_{1.04}Si_{1.27}Al_{1.27}(O,N^{0-30})$ (i.e. 0–30 eq% N). A Y : Si : Al ratio of 5 : 3 : 2 was established, but no X-ray data were reported.

Part of the yttrium sialon glass-forming region has been investigated by Dinger and co-workers[6] who studied the crystallisation of glasses near the Y_2O_3–SiO_2–AlN plane. This work involved mainly the formation of y- and δ-yttrium silicates, but an additional phase was observed at temperatures around 1200°C which the authors calculated to have the composition $YSi_2AlO_4N_2$. Electron diffraction data suggested an orthorhombic unit cell with dimensions a = 23·1 Å, b = 5·01 Å, c = 8·06 Å. The high nitrogen content of this phase was explained by the abundance of silicates forming from the original composition of $Y_{0.26}Si_{0.30}Al_{0.11}ON_{0.11}$.

Analysis of the crystalline products resulting from heat treatment studies in the yttrium and rare earth sialon systems has revealed that phase relationships and their stability ranges are dependent not only on temperature and composition but also on cation size; while some phases are stable throughout the whole lanthanide series (e.g. $M_5Si_3O_{12}N$ (apatite), $M_4Si_2O_7N_2$ (J-phase)), others are stable for either the larger (~La–Dy) or the smaller (~Dy–Lu) cations,

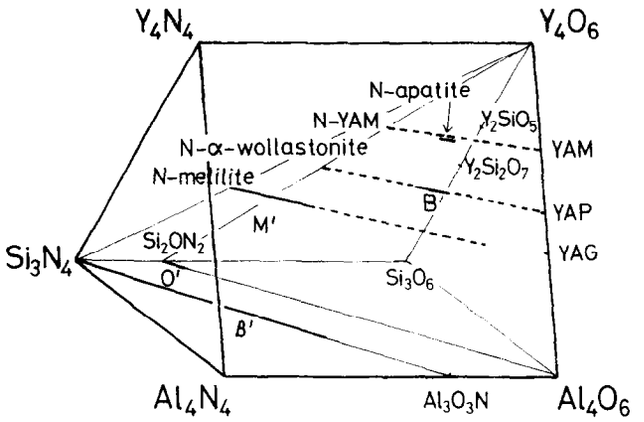

Fig. 1. Crystalline phases in the Y–Si–Al–O–N system.

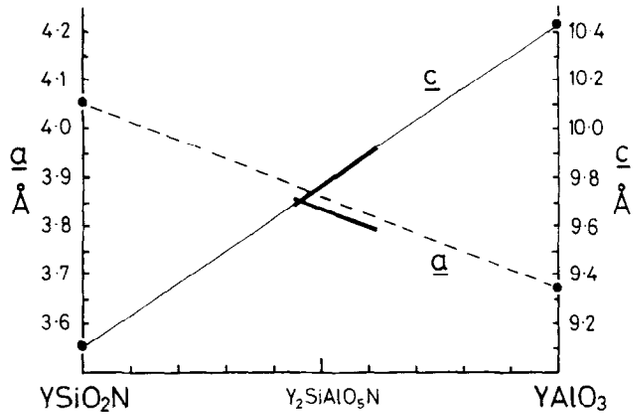

Fig. 2. Unit cell dimensions for B-phase in the range $YSiO_2N$–$YAlO_3$.

but not throughout the whole series. Examples of the larger cation phases are: $MSiO_2N$, M = La–Gd (wollastonite);[2] $M_3Si_3Al_3O_{12}N_2$, M = La–Dy (U-phase);[8] $M_4Si_9Al_5O_{30}N$, M = La–Nd, (W-phase);[9,10] smaller cation series are: $M_3Al_5O_{12}$, M = Dy–Lu (garnet) and M_2SiAlO_5N, M = Dy–Lu, (B-phase).[9] From these data it can be seen that Dy lies at the unstable end of several of the series and since Y has an ionic radius (0·9 Å) close to Dy, it is expected, and has indeed been shown, that yttrium would also occur in phases at both ends of the rare earth series, with limited stability in some cases. Hence there is more possibility of finding new oxynitridie phases in the Y–Si–Al–O–N (or mid Ln) system than at either end of the Ln–Si–Al–O–N systems.

2 Experimental

Samples were prepared by melting compositions from appropriate mixtures of the following powders: Si_3N_4 (Grade LC10 — HC Starck, Berlin); Al_2O_3 (Grade A17 — Alcoa Chemie Gmbh); SiO_2 (Analar Grade — BDH Chemical Ltd); $(Y,Ln)_2O_3$ (99·9% — Rare Earth Products). Powders were mixed by hand in isopropanol and uniaxially pressed into 5–20 g pellets; these were melted at 1650–1750°C in N_2 in a graphite element furnace or a graphite induction furnace for 30 min using a graphite crucible lined either with BN alone or with a 50/50 BN/Si_3N_4 powder mix.

Heat treatment was carried out in a molybdenum-wound vertical furnace, or a silicon carbide horizontal furnace in N_2 at various temperatures in the range 1000–1400°C. Crystalline products were identified by means of a Hägg-Guinier focusing camera and Cu $K\alpha_1$ or Fe $K\alpha_1$ radiation, the latter being particularly helpful for Dy-containing samples, since the intensity of fluorescent scattering is high with Cu radiation but negligible with Fe. Subsequent microstructural studies were carried out on a Camscan S4-80DV scanning electron microscope equipped with a Link energy dispersive X-ray analysis (EDX) system. Electron diffraction patterns were obtained using transmission electron microscopy using a JEM 100CX instrument.

3 Results

3.1 I_w-phase

This phase, I_w, was first observed using SEM techniques by Leng-Ward and Lewis[4,5] as a result of heat treating yttrium sialon glass samples, particularly those with composition $Y_{1\cdot04}Si_{1\cdot27}Al_{1\cdot27}(O, N^{0-30})$ (i.e. 0–30 eq% N). No X-ray data were reported, but a Y : Si : Al ratio of 5 : 3 : 2 was determined. Preliminary preparations at Newcastle[10] gave very characteristic microstructures (Fig. 3) and strong lines close to B-phase positions, but the X-ray diffraction pattern often showed B-phase as a major constituent, so that I_w was thought to be merely a second B-phase, consistent with Leng-Ward's EDX composition and lying on the same line of cation ratio Y : (Si,Al) 1 : 1 (with residual glass). Speculative glass compositions

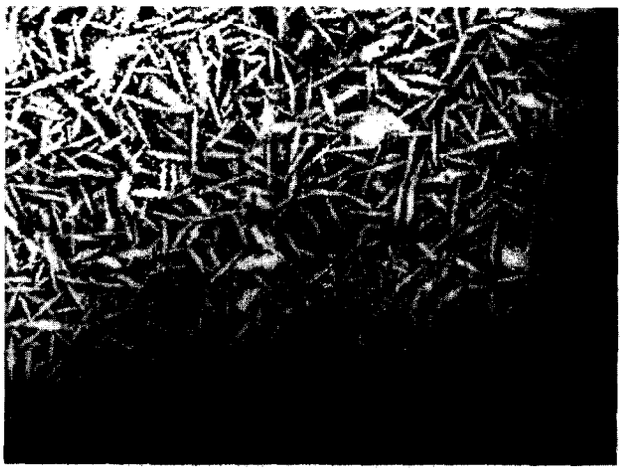

Fig. 3. Back-scattered electron image of I_w-phase.

$Ln_3Si_3Al_3(O,N^{5,10})$ where Ln = Nd, Dy, Yb were prepared and heat treated at 1150°C to determine whether this phase extends into the lanthanide series; no equivalent was found. The purest sample of I_w obtained in the present work, i.e ~90% with Q-phase and a trace of YAG, was from the starting composition $Y_3Si_3Al_2O_{12\cdot15}N_{0\cdot90}$ (10 eq% N) heat treated at 1150°C for 64 h, and X-ray diffraction data are listed in Table 1. Examination of the positions of the strongest lines shows a hexagonal-type sub-cell similar to B-phase (Table 2) and the wollastonites and if the mean position of doublets is used, unit cell dimensions of this sub-cell correspond to a = 3·781, c = 10·06 Å. Figure 2 shows the variation of sub-cell dimensions with (Si,Al) and (O,N) substitution and if the measured values are plotted they correspond exactly on this graph to the composition of $Y_2Si_{0\cdot57}Al_{1\cdot43}O_{5\cdot43}N_{0\cdot57}$. This composition, with an Si : Al ratio of approximately 3 : 7, is quite different from that proposed by Leng-Ward and Lewis[4,5] which is 6 : 4. The nitrogen content (10 eq%) in the starting mixture, however, is in better agreement, i.e. from the unit cell plot the present samples give 14 eq% N, while Leng-Ward reckoned 5–10 eq% N. When taking into account the other phases occurring during heat-treatment experiments,[11] either Si : Al ratio (3 : 7 or 6 : 4) is feasible, such that when B or I_w phases decompose, wollastonite and YAG remain. EDX analysis carried out on this sample shows a Y : Si : Al ratio of 4·5 : 3·5 : 2 which is close to Leng-Ward's analysis of 5 : 3 : 2. It would appear. therefore, that the composition of I_w does not lie on the $YSiO_2N$–Y_2SiAlO_5N–$YAlO_3$ line, and

Table 1. X-ray diffraction data for I_w-phase, $Y_n(Si,Al)_3(O,N)_9$

hkl	d_{calc}	d_{obs}	I_{obs}	*hkl*	d_{calc}	d_{obs}	I_{obs}
100	11·07	11·04	13	43$\bar{1}$	2·151	2·151	<1
001	9·858	9·867	2	430	2·133	2·132	<1
011	7·037	7·032	1	34$\bar{1}$	2·077	2·077	<1
101	6·752	6·720	1	340	2·077		
200	5·534	5·548	<1	323	2·054	2·053	1
020	5·025	5·024	25	043	1·996	—	—
002	4·929	4·929	2	34$\bar{2}$	1·991	1·990	57
10$\bar{2}$	4·859	4·853	<1	341	1·990		
210	4·848			30$\bar{5}$	1·895	—	—
120	4·576	4·574	1	304	1·890	1·891	44
021	4·477	4·475	2	60$\bar{1}$	1·879	1·879	9
201	4·476			31$\bar{5}$	1·862	1·862	1
12$\bar{1}$	4·281	4·289	1	314	1·857	—	—
102	4·215	4·209	<1	61$\bar{1}$	1·847	1·845	2
121	4·031	4·034	1	325	1·773	1·779	2
220	3·720	3·723	1	324	1·769	1·769	25
30$\bar{1}$	3·693	3·688	1	62$\bar{1}$	1·760	1·759	3
300	3·689			053	1·715	—	—
22$\bar{1}$	3·637	3·637	2	35$\bar{2}$	1·712	1·711	1
022	3·519	3·517	5	351	1·711		
221	3·342	3·337	1	060	1·675	1·675	1
003	3·286	3·277	26	33$\bar{5}$	1·649	1·654	1
30$\bar{2}$	3·266	3·266	26	334	1·646	—	—
301	3·258			006	1·643	1·640	4
031	3·172	3·172	<1	63$\bar{1}$	1·639		
22$\bar{2}$	3·170			60$\bar{4}$	1·633	1·631	3
013	3·123	3·115	10	602	1·329	1·628	1
31$\bar{2}$	3·106	3·104	15	016	1·621	1·619	1
311	3·099			61$\bar{4}$	1·612	1·612	3
131	3·001	3·005	1	612	1·608	—	—
32$\bar{1}$	2·976	2·974	1	026	1·562	1·559	7
320	2·974			62$\bar{4}$	1·553	1·555	<1
113	2·873	2·876	1	622	1·550	1·552	13
12$\bar{3}$	2·774	2·775	1	34$\bar{5}$	1·513	1·514	1
023	2·750	2·747	100	344	1·510	1·509	17
32$\bar{2}$	2·738	2·735	100	64$\bar{1}$	1·505	1·505	6
321	2·734			063	1·492	1·492	7
31$\bar{3}$	2·629	2·630	<1	36$\bar{2}$	1·490	1·490	20
040	2·513	2·513	25	361	1·490		
004	2·646	2·462	1	036	1·475	1·471	1
140	2·450	2·451	<1	63$\bar{4}$	1·468		
42$\bar{1}$	2·450			632	1·465		
322	2·390	2·390	<1	046	1·375	1·373	7
331	2·336	2·336	1	64$\bar{4}$	1·369	1·370	1
303	2·251	2·252	<1	642	1·367	1·369	10

Monoclinic: a = 11·2729 Å, b = 10·0503 Å, c = 10·0405 Å, β = 100·95°.

Table 2. X-ray diffraction data for B-phase, Y_2SiAlO_5N

hkl	d_{obs}	I_{obs}	*hkl*	d_{obs}	I_{obs}
002	4·8748	26	114	1·5083	15
100	3·3291	55	106	1·4593	16
101	3·1474	18	204	1·3739	13
102	2·7484	100	107	1·2806	1
004	2·4358	18	210	1·2579	6
103	2·3241	1	211	1·2473	<1
104	1·9651	42	116	1·2402	2
110	1·9211	39	008 }	1·2182	21
112	1·7873	24	212 }		
105	1·6804	1	206	1·1625	8
200	1·6637	7	108	1·1444	5
201	1·6393	1	214	1·1181	17
202	1·5741	16	300	1·1097	3

Hexagonal: a = 3·8421(4) Å, c = 9·7464(10) Å.

that the wollastonite-type of structure, albeit increasingly distorted, must extend into an additional dimension towards lower nitrogen-containing compositions while preserving the higher Si : Al ratio.

Figure 4 shows the hexagonal sub-cell of B-phase with the unit cell parameter of 3·78 Å represented by the distance between the lattice points; the third dimension of 10 Å lies perpendicular to this plane. If the unit cell is extended to more than one basic unit in the (001) plane, the weak superlattice lines of I_w-phase index on the monoclinic cell (dotted) of approximate dimensions a = 11·28 Å, b = 10·07 Å, c = 10·02 Å, β = 101·0°, i.e. a multiple of three units in each direction. A small variation in unit cell dimensions is observed between samples and those quoted in Table 1 are a = 11·2729, b = 10·0503, c = 10·0405 Å, β = 100·95°; examination of indexing for absent reflections shows only 0k0 lines (k odd) missing, establishing a space group of $P2_1$. Due to the low intensity of superlattice lines on the diffraction pattern and the number of overlapping reflexions, only the strongest lines corresponding to the hexagonal cell are listed below 2·0 Å.

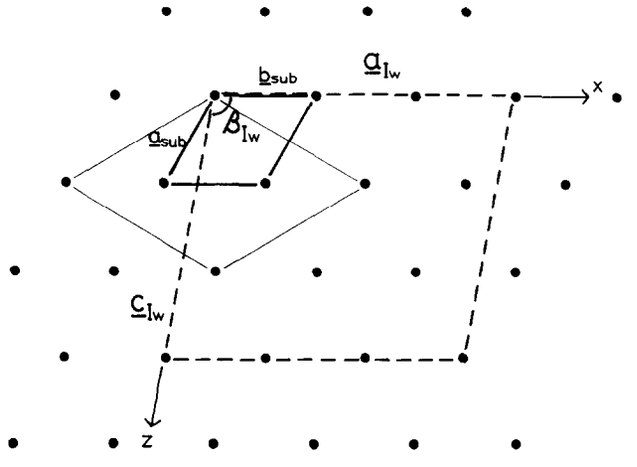

Fig. 4. Unit cell of I_w-phase with pseudo-hexagonal lattice.

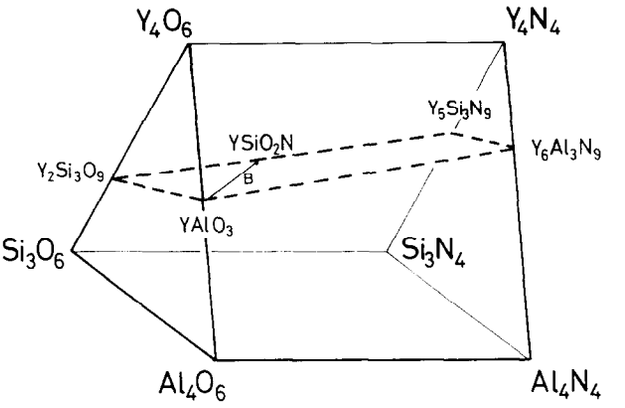

Fig. 5. $Y_n(Si,Al)_3(O,N)_9$ plane in the Jänecke prism.

There remains yet some speculation into the composition of I_w-phase. Since the sialon wollastonite structures all consist of three-membered $(Si,Al)_3(O,N)_9$ rings separated by layers of larger cations,[7] the similarity of the diffraction pattern of I_w would suggest some variation of this arrangement. Figure 5 shows the position of the $Y_n(Si,Al)_3(O,N)_9$ plane in the Jänecke prism; an oxygen-rich wollasonite-type composition would therefore lie in the triangle $YSiO_2N$–$YAlO_3$–$Y_2Si_3O_9$. If the $(Si,Al)_3(O,N)_9$ ring structure is to be preserved, for any given Si : Al ratio the charge difference resulting from oxygen substitution for nitrogen can be compensated for by a reduction in yttrium. Since the total unit cell contents of the B-phase sub-cell are Y_2SiAlO_5N, those of I_w must be a maximum of nine times this sub-cell (Fig. 4), i.e. $Y_{18}(Si,Al)_{18}(O,N)_{54}$. On considering the two EDX Si : Al ratios 3 : 2 and 3·5 : 2 and a nominal nitrogen content of 10 eq%, these would give compositions $Y_{15.64}Si_{10.8}Al_{7.2}O_{50.28}N_{3.72}$ and $Y_{15.42}Si_{11.46}Al_{6.54}O_{50.28}$-

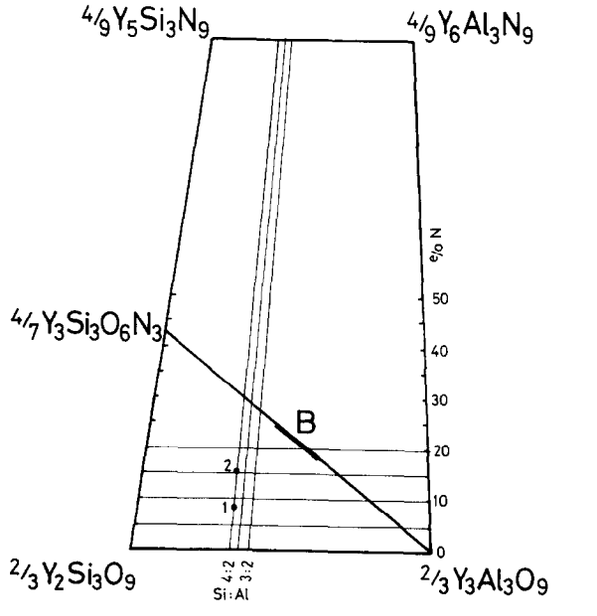

Fig. 6. $Y_n(Si,Al)_3(O,N)_9$ plane showing possible I_w compositions: (1) $Y_{15}Si_{12}Al_6O_{51}N_3$ and (2) $Y_{16}Si_{12}Al_6O_{48}N_6$.

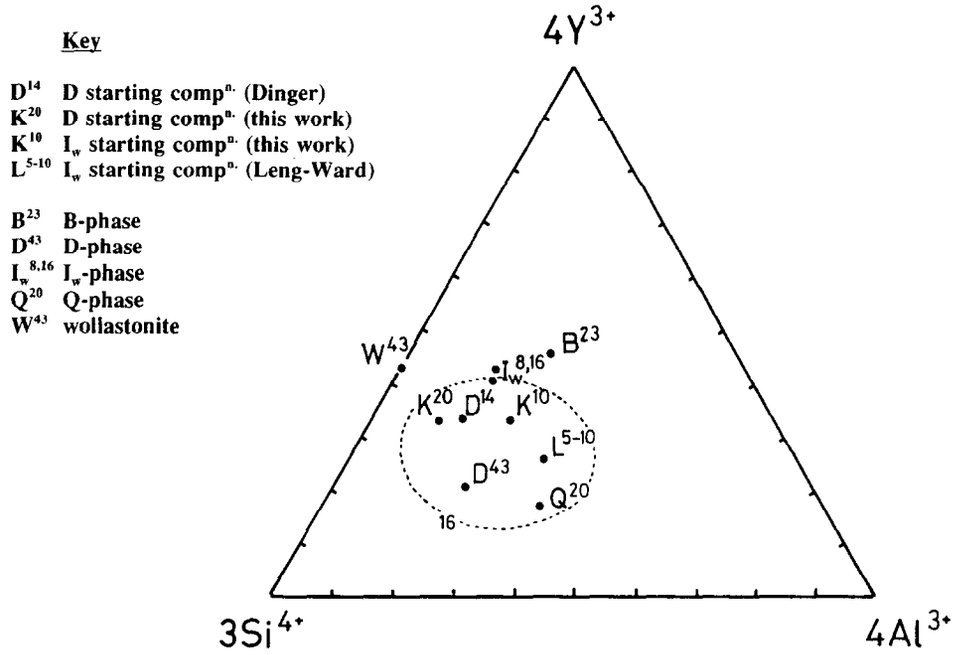

Fig. 7. Starting and final compositions of I_w, Q and D phases (eq% N superscripted).

$N_{3.72}$ respectively. Using integer approximations for such expressions, two possible compositions result:

(1) $Y_{15}Si_{12}Al_6O_{51}N_3$ (8·11 eq% N) and

(2) $Y_{16}Si_{12}Al_6O_{48}N_6$ (15·79 eq% N)

These are plotted on Fig. 6, a representation of the $Y_n(Si,Al)_3(O,N)_9$ plane showing lines of selected Si : Al and O : N ratios, and also on Fig. 7 which shows the starting and final compositions (eq% N superscripted) of each of the phases discussed in this work. Relative to the wollastonite structures either three or two of the yttrium sites remain unoccupied. Preparative techniques must be optimised and further structural data collected before a full structure determination of I_w-phase can be carried out.

3.2 Q-phase

This phase was first observed during post-preparative heat treatment[10,12] of β or α–β sialon compositions densified with rare earth additives; designated Q, it formed alongside B-phase, YAG or U-phase at 1000–1150°C. In these products the maximum amount observed was about 30%, depending on the system, but mixed Y_2O_3 + Dy_2O_3 additions gave the most stable product, i.e. up to 1250°C. A typical microstructure of yttrium Q-phase heat treated at 1100°C is shown in Fig. 8.

Subsequent observations have been made during the heat treatment of compositions lying on the 20 eq% N plane in the Y–Si–Al–O–N system, when this phase was prepared apparently pure except for an unknown small amount of residual glass. It occurs near the composition $YSi_2Al_2O_{6\cdot8}N_{1\cdot13}$; small deviations from this starting mixture show a decrease in the Q-phase content in all cases, confirming a point composition. EDX analysis also suggests a cation ratio Y : Si : Al of about 1 : 2 : 2, although the nitrogen content may be greater than 20 eq% N, which would explain accompanying traces of mullite or yttrium silicate. Figure 7 shows the glass-forming region on the 16 eq% N plane in the Jänecke prism; the Q-phase composition (Q^{20}) is shown. The same composition has been prepared in other rare earth systems to explore its stability; Q-phase was found to be present in the smaller rare earth samples (Ln=Dy–Yb), but not in the larger cation-containing (La–Gd) systems where U-phase predominates. As mentioned previously U-phase is stable in the rare earth series from La to Dy,[8] and YAG occurs from Dy to Yb. However, since Y and Dy lie at the unstable end of each of these ranges, Q-phase is more easily

Fig. 8. Back-scattered electron image of yttrium Q-phase.

Table 3. X-ray diffraction data for Q-phase, $YSi_2Al_2O_{6\cdot8}N_{1\cdot13}$

d_{obs}	$sin^2\theta$	I_{obs}	d_{obs}	$sin^2\theta$	I_{obs}	d_{obs}	$sin^2\theta$	I_{obs}
8·1948	0·00884	100	2·1940	0·12327	2	1·5199	0·25684	62
6·6396	0·01346	6	2·1807	0·12477	30	1·5091	0·26053	27
5·4097	0·02028	2	2·1108	0·13318	43	1·4993	0·26397	13
4·5601	0·02853	6	2·0485	0·14140	10	1·4943	0·26574	15
4·0964	0·03536	5	2·0283	0·14423	16	1·4703	0·27447	19
3·8371	0·04030	6	2·0192	0·14553	21	1·4652	0·27639	3
3·7414	0·04239	13	1·9601	0·15444	25	1·4391	0·28649	2
3·3239	0·05371	87	1·9354	0·15841	5	1·4377	0·28706	3
3·2108	0·05755	1	1·9194	0·16105	7	1·4291	0·29054	20
3·0821	0·06246	78	1·8884	0·16640	21	1·4023	0·30175	8
3·0309	0·06459	1	1·8643	0·17072	7	1·3816	0·31087	2
2·9343	0·06891	15	1·8413	0·17501	4	1·3715	0·31545	6
2·8788	0·07160	1	1·8293	0·17732	15	1·3650	0·31848	27
2·7410	0·07897	6	1·8105	0·18105	24	1·3601	0·32077	11
2·7313	0·07954	22	1·7849	0·18624	17	1·3512	0·32498	8
2·7195	0·08023	56	1·7780	0·18769	4	1·2998	0·35121	4
2·6140	0·08683	51	1·7689	0·18964	11	1·2986	0·35184	5
2·5820	0·08900	82	1·7444	0·19500	15	1·2907	0·35618	7
2·5114	0·09408	15	1·6650	0·21404	47	1·2799	0·36220	7
2·4913	0·09560	8	1·6555	0·21651	2	1·2725	0·36646	8
2·4452	0·09924	19	1·6386	0·22098	1	1·2459	0·38224	3
2·3206	0·11019	4	1·6291	0·22358	8	1·2259	0·39481	4
2·2892	0·11322	3	1·6238	0·22505	14	1·2246	0·39569	2
2·2804	0·11410	2	1·6122	0·22830	8	1·2236	0·39629	6
2·2039	0·12216	23	1·5562	0·24500	8	1·2105	0·40492	19

detectable in these systems. Although the strong lines of the X-ray patterns are obvious in the different rare earth systems, the weakest lines are more difficult to define with certainty. Data have been collected for Y, Dy, Er and Yb products using both Cu and Fe radiation in order to reduce the fluorescent scattering in the most susceptible products, particularly Dy, and the diffraction pattern of the yttrium sample is shown in Table 3. Attempts to index the X-ray pattern of Q-phase have proved hitherto unsuccessful.

3.3 D-phase

This phase was first observed on heat-treatment of yttrium sialon glasses of Y : Si : Al atomic ratio 28 : 42 : 16 containing 17 or 20 eq% N. As with Q-phase, several more related compositions were prepared and heat-treated at various temperatures to maximise the proportion of D-phase present in the material. A typical starting composition of a product containing a significant amount of D (K^{20}) is shown in Fig. 7; Dinger's starting composition is marked D^{14}. It was seen from X-ray results after heat-treatment at 1150°C that D-phase coexists usually with y-$Y_2Si_2O_7$, or occasionally with another silicate such as the δ- or β- form. Where these are the only crystalline products, D would appear to be rich in nitrogen (perhaps approaching 40 eq%) since most of the starting compositions contain 20 eq% N; however in many cases there also occur nitrogen-containing phase(s), which would lower the apparent nitrogen content of D-phase. It was not possible to establish the cation ratio Y : Si : Al since the grain size was too small for EDX analysis to be meaningful. Nevertheless, a reasonably reliable diffraction pattern has been obtained (Table 4 (^{y}=overlap with y-$Y_2Si_2O_7$)), which is quite distinct from the accompanying very diffuse y-$Y_2Si_2O_7$ pattern. Because of the strong line at 11·6 Å this phase may be misinterpreted as I_w-phase, but both have been found to coexist after heat treatment at 1150°C for 1000 h. Indexing of the diffraction pattern has not yet been achieved although two dimensions of 23·1 and 5·01 Å are in good agreement with those reported by Dinger *et al.*;[6] the third dimension could not be confirmed by recent calculations. Dinger's phase was formed from a glass of composition $Y_{0\cdot26}Si_{0\cdot30}Al_{0\cdot11}ON_{0\cdot11}$, containing 14 eq% N, from which y- and δ- yttrium silicates also formed during heat-treatment. These authors calculated the composition of D to be $YSi_2AlO_4N_2$ (43 eq% N); this lies outside the glass-forming region and produces Si_3N_4 and B-phase with glass on initial firing. Heat treatment at 1150°C for 12 h gives I_w and B phases and no D-phase. The calculated composition has a Y : Si : Al ratio very similar to that of W-phase[9,10] in the rare earth systems, albeit with very different O : N; it is possible therefore that the structures of D- and W- phases are related in some way whilst remaining distinct from one another.

Table 4. X-ray diffraction data for D-phase, $YSi_2AlO_4N_2$

d_{obs}	$sin^2\theta$	I_{obs}	d_{obs}	$sin^2\theta$	I_{obs}	d_{obs}	$sin^2\theta$	I_{obs}
11·6	0·00444	100	2·2481	0·11740	13	1·6591	0·21555	19
6·9624	0·01224	<3	2·2082	0·12169	5	1·6537	0·21697	5
5·3404	0·02081	5	2·1993	0·12267	9	1·6509	0·21771	9
4·8991	0·02472	42	2·1951	0·12315	9	1·6220	0·22555	11
4·5969	0·02808	72	2·0990	0·13468	11	1·5992[y]	0·23202	<10
4·1985	0·03366	3	2·0898	0·13586	45	1·5903[y]	0·23462	39
4·1137	0·03506	21	1·9957	0·14898	<3	1·5631	0·24284	5
3·8512	0·04001	47	1·9494	0·15613	10	1·5608	0·24357	6
3·7976	0·04114	68	1·9372	0·15811	4	1·5569	0·24479	5
3·6894	0·04359	<3	1·9141	0·16195	3	1·5489	0·24733	57
3·6279	0·04508	<3	1·9039	0·16368	<3	1·5461[y]	0·24822	10
3·4352	0·05028	57	1·9001	0·16435	86	1·5426[y]	0·24934	10
3·3956	0·05146	79	1·8688[y]	0·16990	<10	1·5295[y]	0·25364	68
3·2909	0·05479	11	1·8561[y]	0·17224	<10	1·5145	0·25871	54
3·0979	0·06183	5	1·8374	0·17575	5	1·4847	0·26920	43
3·0017	0·06586	100	1·8114	0·18084	4	1·4658	0·27618	13
2·9282	0·06920	80	1·8004	0·18306	4	1·4545	0·28046	29
2·8877	0·07116	7	1·7959	0·18398	12	1·4136	0·29693	5
2·8172	0·07476	60	1·7924	0·18468	7	1·4019	0·30193	4
2·7846	0·07652	13	1·7697	0·18946	5	1·3715	0·31547	72
2·7723	0·07720	6	1·7674	0·18996	4	1·3670	0·31754	5
2·7568	0·07807	32	1·7468[y]	0·19445	<10	1·3657	0·31815	4
2·7035	0·08118	63	1·7353[y]	0·19706	<5	1·3566	0·32244	4
2·6869	0·08219	43	1·7322	0·19776	15	1·3541	0·32362	7
2·6572	0·08404	7	1·7182	0·20098	5	1·3504	0·32536	19
2·5315	0·09259	40	1·7155	0·20163	5	1·3125	0·34445	15
2·5030	0·09471	30	1·6974[y]	0·20593	26	1·3046	0·34861	5
2·4500	0·09885	21	1·6764	0·21113	4	1·2946[y]	0·35405	<5
2·2998	0·11219	20	1·6663	0·21370	17	1·2917	0·35562	4
2·2753	0·11461	<3	1·6643	0·21421	9			

4 Conclusions

From all these crystalline phases described, Q and I_w are glass ceramics, with Q lying well inside the glass-forming region of the Y–Si–Al–O–N or Y–Ln–Si–Al–O–N systems with relatively high Al content, while I_w lies on the edge with almost maximum yttrium content. D and B phases lie outside the glass-forming region. Each phase is very sensitive to small changes in composition, temperature and probably duration of heat treatment, and multiphase products are easily formed on crystallising glass materials. Hence identification and characterisation of any minor phases are necessary in establishing more fully the phase relationships in these sialon systems.

Acknowledgements

The authors wish to acknowledge financial support for this work under the EC BRITE-EURAM programme, contract No. BRE2-CT92-0272.

References

1. Rae, A. W. J. M., Yttrium silicon oxynitrides. PhD Thesis, University of Newcastle upon Tyne, 1976.
2. Spacie, C. J., Characterisation and heat treatment of sialon ceramics. PhD Thesis, University of Newcastle upon Tyne, 1984.
3. Liddell, K., Mandal, H. & Thompson, D. P., *J. Mater. Sci.* (1996) to be published.
4. Leng-Ward, G. & Lewis, M. H., Oxynitride glasses and their glass-ceramic derivatives. In *Glasses and Glass-Ceramics*, ed. M. H. Lewis. London, Chapman & Hall, 1989, 106–155.
5. Leng-Ward, G. & Lewis, M. H., Crystallisation in Y–Si–Al–O–N glasses. *Materials Science & Engineering*, **71** (1985) 101–111.
6. Dinger, T. R., Rai, R. S. & Thomas, G., Crystallization behaviour of a glass in the Y_2O_3–SiO_2–AlN system. *J. Am. Ceram. Soc.*, **71**(4) (1988) 236–244.
7. Korgul, P. & Thompson, D. P., Crystallisation behaviour of N-α-wollastonite glasses. *Brit. Ceram. Proc., Complex Microstructures*, **20** (1989) 69–80.
8. Grins, J., Käll, P. O., Kiddell, K., Korgul, P. & Thompson, D. P., Sialon U-phase; an alternative crystalline grain boundary phase for β sialon ceramics. In *New Materials and their Applications II*, 1990, pp. 427–434.
9. Mandal, H., Thompson, D. P. & Ekström, T., Heat treatment of Ln–Si–Al–O–N glasses. In *Materials for Advanced Technology Applications*, ed. M. Buggy & S. Hampshire. Trans Tech Publications, Zurich, 1991, pp. 187–204.
10. Mandal, H. & Thompson, D. P., New oxynitride glass ceramics. In *II International Ceramic Congress Proceedings, Vol 1 — Traditional Ceramics*, ed. M. L. Öveçoğlu & H. Yaparlar. Turkish Ceramic Society, 1994, pp. 366– 377.
11. Liddell, K. & Thompson, D. P., to be published.
12. Mandal, H., Thompson, D. P. & Ekström, T., Heat treatment of sialon ceramics densified with higher atomic number rare earth and mixed yttrium/rare earth oxides. In *Special Ceramics 9*, London, 1990, ed. R. Stevens. Institute of Ceramics, UK, 1992, pp. 97–104.